

# Effects of Substrate Stiffness on Cell Morphology, Cytoskeletal Structure, and Adhesion

Tony Yeung,<sup>1</sup> Penelope C. Georges,<sup>1</sup> Lisa A. Flanagan,<sup>2</sup> Beatrice Marg,<sup>2</sup>  
Miguelina Ortiz,<sup>1</sup> Makoto Funaki,<sup>1</sup> Nastaran Zahir,<sup>1</sup> Wenyu Ming,<sup>1</sup>  
Valerie Weaver,<sup>1</sup> and Paul A. Janmey<sup>1,2\*</sup>

<sup>1</sup>*Institute for Medicine and Engineering, University of Pennsylvania, Philadelphia*

<sup>2</sup>*Hematology Division, Brigham and Women's Hospital, Boston, Massachusetts*

The morphology and cytoskeletal structure of fibroblasts, endothelial cells, and neutrophils are documented for cells cultured on surfaces with stiffness ranging from 2 to 55,000 Pa that have been laminated with fibronectin or collagen as adhesive ligand. When grown in sparse culture with no cell-cell contacts, fibroblasts and endothelial cells show an abrupt change in spread area that occurs at a stiffness range around 3,000 Pa. No actin stress fibers are seen in fibroblasts on soft surfaces, and the appearance of stress fibers is abrupt and complete at a stiffness range coincident with that at which they spread. Upregulation of  $\alpha 5$  integrin also occurs in the same stiffness range, but exogenous expression of  $\alpha 5$  integrin is not sufficient to cause cell spreading on soft surfaces. Neutrophils, in contrast, show no dependence of either resting shape or ability to spread after activation when cultured on surfaces as soft as 2 Pa compared to glass. The shape and cytoskeletal differences evident in single cells on soft compared to hard substrates are eliminated when fibroblasts or endothelial cells make cell-cell contact. These results support the hypothesis that mechanical factors impact different cell types in fundamentally different ways, and can trigger specific changes similar to those stimulated by soluble ligands. *Cell Motil. Cytoskeleton* 60:24–34, 2005. © 2004 Wiley-Liss, Inc.

**Key words:** substrate stiffness; cell morphology; fibroblasts; mechanosensing; cell-matrix interaction; actin cytoskeleton; integrin expression

## INTRODUCTION

Most cells in multicellular organisms are attached to much softer materials than the glass and plastic surfaces on which nearly all studies are done in vitro. The most common attachment site for a mammalian cell is another similar cell or the extracellular matrix, and these materials have elastic moduli on the order of 10 to 10,000 Pa [Bao and Suresh, 2003; Wakatsuki et al., 2000]. Forces generated by cytoskeletal motors applied to membrane attachment sites can deform materials with this range of stiffness but cannot move an attachment site on a rigid surface. Consequently, cell morphology and functions can depend strongly on substrate stiffness under conditions where chemical signals are constant. The acute signal and

transcriptional changes mediating cells' responses to stiffness are beginning to be characterized.

Previous studies using fibroblasts have shown that cells generate more traction force and develop a broader and flatter morphology on stiff substrates than they do on

\*Correspondence to: Paul Janmey, Institute for Medicine and Engineering (IME), University of Pennsylvania, 1010 Vagelos Laboratories, 3340 Smith Walk, Philadelphia, PA 19104.  
E-mail: janmey@mail.med.upenn.edu

Received 22 April 2004; accepted 27 August 2004

Published online in Wiley InterScience (www.interscience.wiley.com).

DOI: 10.1002/cm.20041

soft but equally adhesive surfaces and that cells will preferentially migrate from a soft to a hard surface [Lo et al., 2000]. Cell growth and survival also depend on substrate stiffness, as gelatin-coated materials softer than 100 Pa do not support survival of non-transformed cells but do support growth of transformed cell types [Wang et al., 2000a]. Large changes in the extent of protein tyrosine phosphorylation and cytoskeletal structure correlate with stiffness, and are presumably part of the stiffness-sensing apparatus [Pelham and Wang, 1997]. Responses to mechanical stimuli may be cell-type specific. Motor neurons derived from embryonic mouse spinal cord extend neurites with extensive branches on soft but not hard surfaces [Flanagan et al., 2002]. In contrast, smooth muscle cells, like fibroblasts, extend processes more avidly on hard surfaces and are rounded on soft materials [Engler et al., 2004].

In this study, we extend the range of cell types examined on materials with well-controlled stiffness by employing protein-laminated polyacrylamide gels to study GFP-actin and GFP- $\alpha 5$  integrin-expressing NIH 3T3 fibroblasts, bovine aorta endothelial cells, and human neutrophils. The results show that the morphologies of different cell types differ both quantitatively and qualitatively with substrate stiffness, that the stiffness response depends on the nature of the adhesion ligand bound to the surface, and that changes in stiffness can initiate specific transcription events leading to upregulation of adhesion receptors.

## MATERIALS AND METHODS

### Preparation of Glass Cover Slips

The substrate is prepared by allowing polyacrylamide solutions to polymerize between two chemically modified glass cover slips. Briefly, 200  $\mu$ L of a 0.1 N NaOH solution is pipetted to cover the surface of a 25-mm-diameter glass cover slip (Fisherbrand, catalog no. 12-545-102; Fisher Scientific, Pittsburgh, PA) for 5 min. The NaOH solution is then aspirated, and 200  $\mu$ L of 3-APTMS (3-Aminopropyltrimethoxysilane, Sigma no. 28-1778, Sigma, St. Louis, MO) is applied for 3 min. The glass cover slip is thoroughly rinsed with de-ionized water to wash away any remaining 3-APTMS solution. Then, 200  $\mu$ L of 0.5%v glutaraldehyde (Sigma no. G7651) in  $H_2O$  is added onto the cover slip for 20 min. The glass cover slip is subsequently rinsed with water. An 18-mm-diameter glass cover slip is placed on top of a piece of parafilm inside a tissue culture dish. A small amount of a 10% by volume Surfasil solution (Pierce no. 42800, Pierce, Rockford, IL) in chloroform is pipetted onto the parafilm near the cover slip. The tissue culture dish with a half-closed lid is placed inside a vacuum desiccator for 10 min.

### Preparation of Polyacrylamide Gel

A 30% w/v acrylamide stock solution is prepared by mixing 15 g of acrylamide powder (FisherBiotech CAS no. 79061) with 35 mL of deionized  $H_2O$ . A 1% w/v bis-acrylamide stock solution is prepared by mixing 500 mg bis-acrylamide powder (FisherBiotech CAS no. 110269) with 49.5 mL  $H_2O$ . Polyacrylamide gel solutions are prepared with acrylamide at final concentrations of 3, 5, 7.5, or 12% w/v and bis-acrylamide from 0.05 to 0.6% w/v. To polymerize the solution, 1.5  $\mu$ L TEMED (FisherBiotech CAS no. 110189) and 5  $\mu$ L of 10% ammonium persulfate are added with the appropriate amount of  $H_2O$  to yield a final volume of 1,000  $\mu$ L. A fixed volume of 45  $\mu$ L of the polyacrylamide solution is immediately pipetted onto the center of the 25-mm-diameter glass cover slip. The 18-mm-diameter cover slip is then carefully placed on top of the polyacrylamide solution. The polymerization is completed in about 10 min and the top coverslip is slowly peeled off. The bottom cover slip with the attached polyacrylamide gel is immersed in a multi-well plate (6 Well Cell Culture Cluser, Costar 3516, Corning Inc., Corning, NY) with 3 mL PBS. Polyacrylamide gels with a wide range of shear storage moduli,  $G'$ , can be prepared using the concentration scheme described above. The most flexible gel with 3% w/v acrylamide and 0.05% w/v bis-acrylamide has a shear elastic modulus ( $G'$ ) of 2 Pa while the stiffest gel with 12% w/v acrylamide and 0.60% w/v bis-acrylamide yields a  $G'$  of 55,000 Pa.

### Crosslinking of Adhesion Proteins

A heterobifunctional crosslinker, sulfo-SANPAH (sulfosuccinimidyl6(4'-azido-2'-nitrophenyl-amino)hexanoate, Pierce no. 22589), is used to crosslink extracellular matrix molecules onto the surface of the gel. A small amount (about 1 mg/ml) of sulfo-SANPAH is dissolved in  $H_2O$ , and 200  $\mu$ L of this solution is pipetted onto the gel surface. The polyacrylamide gel is then placed 6 inches under an ultraviolet lamp and irradiated for 10 min. It is then washed three times each with 3 mL of 200 mM HEPES at pH 8.6. After the last HEPES solution is aspirated, 200  $\mu$ L of a 0.14 mg/ml fish fibronectin solution (Sea Run Holdings, South Freeport, ME) [Wang et al., 2000b] or 0.14 mg/ml type I collagen is pipetted on top of the polyacrylamide gel. The multi-well plate housing the gels is then incubated at 5°C for at least 4 h.

### Viscoelastic Characterization

The viscoelastic properties of polyacrylamide gels were quantified by measuring the dynamic shear moduli using an RFS II fluids spectrometer (Rheometrics Inc., Piscataway, NJ). A 500- $\mu$ L sample was polymerized

between two 25-mm stainless steel parallel plates with a corresponding sample thickness of approximately 1 mm. The shear storage modulus  $G'$ , corresponding to the elastic resistance of the gels, was determined from the shear stress in phase with an oscillatory (1 rad/s) shear strain of 2% maximal amplitude, by standard techniques. Similar measurements were conducted using cone and plate geometries where the thickness of the sample was between 50–200  $\mu\text{m}$ , similar to that of gels on which cells are grown, and nearly identical  $G'$  were recorded (data not shown).

### Cell Culture

GFP-actin expressing NIH-3T3 mouse fibroblasts prepared as previously described [Cunningham et al., 2001] were incubated in Dulbecco's Modified Eagle Medium (Cellgro no. 10-013CV) with high glucose, L-glutamine, no sodium pyruvate, phenol red, and 10% bovine calf serum (Hyclone Cat No. SH30072.03 Lot No. AJH10711 Bottle No. 1007, Hyclone, Logan, UT) at a 5%  $\text{CO}_2$  environment.

Bovine aortic endothelial cells were kindly provided by Peter Davies, and incubated in DMEM with high glucose, L-glutamine, no sodium pyruvate, phenol red, and 10% bovine calf serum at a 5%  $\text{CO}_2$  environment.

Human blood neutrophils were isolated from whole blood from healthy volunteers. Collected blood samples were immediately transferred to sodium-heparin-containing polypropylene tubes. Neutrophils were isolated by centrifuging 3 mL whole blood through 3 mL Mono-Poly resolving media (ICN Biomedical, Irvine, CA) to resolve a distinct neutrophil layer. Neutrophils were washed two times with Dulbecco's phosphate-buffered saline (DPBS) (Gibco, Gaithersburg, MD), and contaminating erythrocytes lysed by 40-sec incubation in sterile distilled water. Final neutrophil pellets were resuspended in RPMI 1640 medium (Gibco, Gaithersburg, MD) and kept on ice prior to plating on substrates.

### Morphological Measurements

Phase contrast and fluorescence microscopy were conducted using a Leica DM IRBE microscope and a Hamamatsu C-4742 digital camera. The multi-well plate was briefly removed from the tissue culture incubator for microscopy work. Area and circumference measurements were obtained by tracing cell boundaries manually using NIH Image software.

### Time-Lapse Movies

A temperature-controlled chamber (Biopetechs FCS2 Chamber) was used for time-lapse movies to maintain temperature at 37°C. Two milliliters of a 10,000 cell/ml solution were injected into the temperature-controlled

chamber using a Bio-Rad Econo-Column pump (Bio-Rad, Richmond, CA). Microscopy began within 3 min after flow was stopped. 3T3 fibroblasts were allowed to grow on either a 180- or 55,000-Pa gel. Cells on the 55,000-Pa gel were incubated with  $\text{CO}_2$  independent medium (GibcoBRL Cat No. 18045-088 Lot No. 1099754) with 10% bovine calf serum to maintain physiological pH in the absence of a rich  $\text{CO}_2$  environment. Cells on the 180-Pa gel were incubated with 50%  $\text{CO}_2$  independent medium, 40% DMEM, and 10% bovine calf serum. The rate of cell spreading was analyzed by taking images of sparsely distributed cells at 30-sec intervals.

### Quantification of Integrin Expression

NIH 3T3 GFP-actin expressing fibroblasts grown on polyacrylamide gels with varying stiffnesses for 24 h were used for the quantification of  $\alpha 5$  integrin expression by Western blotting. Polyacrylamide gels on top of the 25-mm glass cover slips were gently scraped off in one piece by a razor blade. The gels were immersed in a Laemmli lysis buffer solution (50 mM Tris-HCL, pH 6.8, 5 mM EDTA, 2% SDS containing 1 mM sodium fluoride, 1 mM sodium orthovanadate, and a cocktail of protease inhibitors) in an Eppendorf tube for 15 min. The cell lysate solution with the addition of non-reducing buffer was then run on an 8% SDS-PAGE gel. The electrophoresis gel was then transferred and blocked using standard protocols. The primary antibody used was  $\alpha 5$  integrin, rabbit sera (Chemicon International, Temecula, CA), and the secondary used was a horseradish peroxidase-linked anti-rabbit IgG polyclonal antibody (Amersham Pharmacia Biotech, Arlington Heights, IL). Protein was detected with an ECL-Plus system (Amersham Pharmacia Biotech). In order to normalize the Western blot result by the number of cells per sample, microscopy was performed to estimate the number of cells grown on each gel substrate before the Western blot procedure. The intensity value of each band after subtraction of the background was then normalized by the number of cells estimated in each sample.

### cDNA Constructs

The  $\alpha 5$  integrin EGFP fusion (generous gift of Rick Horowitz, University of Virginia) [Laukaitis et al., 2001] was excised as a XhoI-NotI fragment from pEGFP-N3 (Clontech, Palo Alto, CA) and subcloned into the retroviral vector Hermes HRS puro GUS (generous gift of Helen Blau, Stanford University, CA) [Rossi et al., 1998] replacing the GUS cDNA between SalI and NotI sites using standard techniques and bringing the fusion under control of a tetracycline (tet) regulated promoter. To produce retrovirus,  $3 \times 10^6$  HEK 293 cells were seeded in gelatin-coated 60-mm dishes, and 24 h later the Hermes HRS puro  $\alpha 5$  integrin EGFP construct was co-

transfected with pVSVG and pCgp (generous gift of Alan Kingsman, Oxford University, UK), which express the VSVG protein and gag-pol genes, respectively, using calcium phosphate. Transfected cells were incubated 8 h at 37°C, media was replaced and returned to 37°C for a further 16 h, after which they were transferred to a 32°C humidified incubator. After 24 h at 32°C media was collected, made 8 µg/ml in polybrene (Sigma), and centrifuged at 3,000g for 5 min to pellet cells and debris. NIH-3T3 cells in a 6-cm dish were incubated with 1.5 ml of retrovirus containing supernatant at 32°C for 8 h, after which the supernatant was replaced with 3 ml of regular media and returned to a 37°C humidified incubator for 36–48 h. Retrovirally transduced cells were selected in media supplemented with 1 µg/ml puromycin until a resistant population grew out. Polyclonality was judged visually by the number of puromycin-resistant colonies and speed of outgrowth, and only pooled populations deemed sufficiently polyclonal were used in experiments. Cells from the pooled population were subsequently infected as above with a high titer MFG-based retrovirus that expresses the tet repressor fused to the HPV16 activation domain (a derivative of the tet off transactivator construct provided by Helen Blau [Rossi et al., 1998], generated in the laboratory of V. Weaver, unpublished data, which has wild type DNA binding activity), prepared by transfection in 293GPG cells (generous gift of Richard Mulligan, Whitehead Institute, MIT, Cambridge, MA) as described in Ory et al. [1996]. Transduced cells were maintained in 1 µg/ml tetracycline to keep  $\alpha 5$  integrin EGFP in the uninduced state. Expression of  $\alpha 5$  integrin EGFP was induced in cells by culturing in the absence of tetracycline in medium containing Tet System Approved FBS (Clontech) for 48 h prior to experiments.

### EGFP Expression Analysis

Cells were directly fixed using 2% paraformaldehyde and visualized using a scanning confocal laser (model 2000-MP; Bio-Rad Laboratories) attached to a fluorescence microscope (Nikon Eclipse TE-300). Confocal images were recorded at 120 $\times$ .

## RESULTS

The large range of physiologically relevant stiffness that can be produced using polyacrylamide gels is shown in Figure 1. The softest gels that can reproducibly be formed and handled for cell studies are made with 3% acrylamide. At low crosslinker concentrations, gels can be produced with elastic moduli below 10 Pa, the consistency of mucus. The upper limit to 3% gels appears to be near 600 Pa. Higher moduli require greater concentrations of acrylamide, and as seen in Figure 1, 5.5 and 7.5% gels allow large variations of elastic moduli as the crosslinker concentration

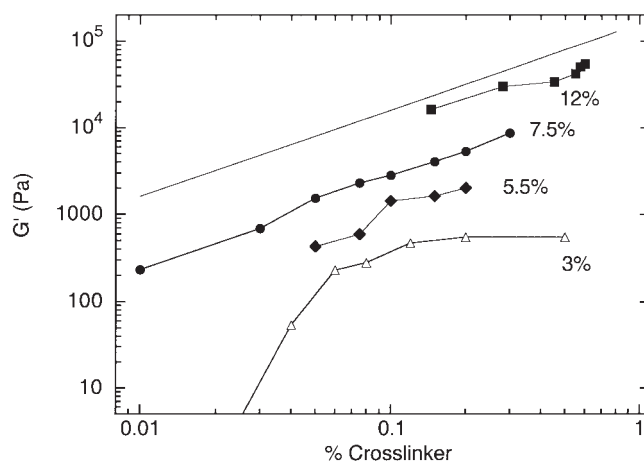


Fig. 1. Mechanical properties of polyacrylamide substrates. The shear modulus of polyacrylamide gels with a range of acrylamide (indicated as percents near data lines) to bis-acrylamide (indicated as crosslinker) proportions was measured. The shear modulus ( $G'$ ), expressed in Pascal, increases at constant polymer mass with increasing crosslinker. Increasing the concentration of acrylamide from 3 to 12% also creates a large stiffness range from 10 to 50,000 Pa. The solid line denotes the theoretical stiffness of a rubberlike network if every crosslink was elastically effective.

is varied. Gels with a concentration above 7.5 % in particular show a remarkably linear dependence of elastic modulus on crosslinker concentration spanning nearly two orders of magnitude in stiffness. For crosslinked rubberlike networks like these acrylamide gels, the elasticity is theoretically predicted to be related to the concentration of crosslinks by the relation

$$G = nRT/V$$

where  $n$  is the number of crosslinks per volume  $V$ , and  $R$  is the gas constant [Flory, 1953]. This theoretical limit, shown by the solid line in Figure 1, is very close to the experimental values measured at high total [polyacrylamide] where each bisacrylamide subunit is most likely to make an elastically effective crosslink.

Figure 2 shows the large dependence of fibroblast morphology on FN-coated gel stiffness. Previous studies have shown that the density of adhesion protein bound to the gel surface is independent of gel stiffness [Flanagan et al., 2002], and imaging of the gel surface with fluorescently labeled FN showed a constant amount of protein bound to both the softest and stiffest gels and a uniformity of coverage that was at least as good as that on plastic (data not shown). The shapes of NIH3T3 fibroblasts after one day in culture range from round, nearly spherical cells with a few irregular protrusions seen on gels of 180 Pa stiffness to large spread cells on gels stiffer than 16,000 Pa, which were indistinguishable from those grown on glass or the plastic surfaces surrounding the gel in the culture dish. As visualized by



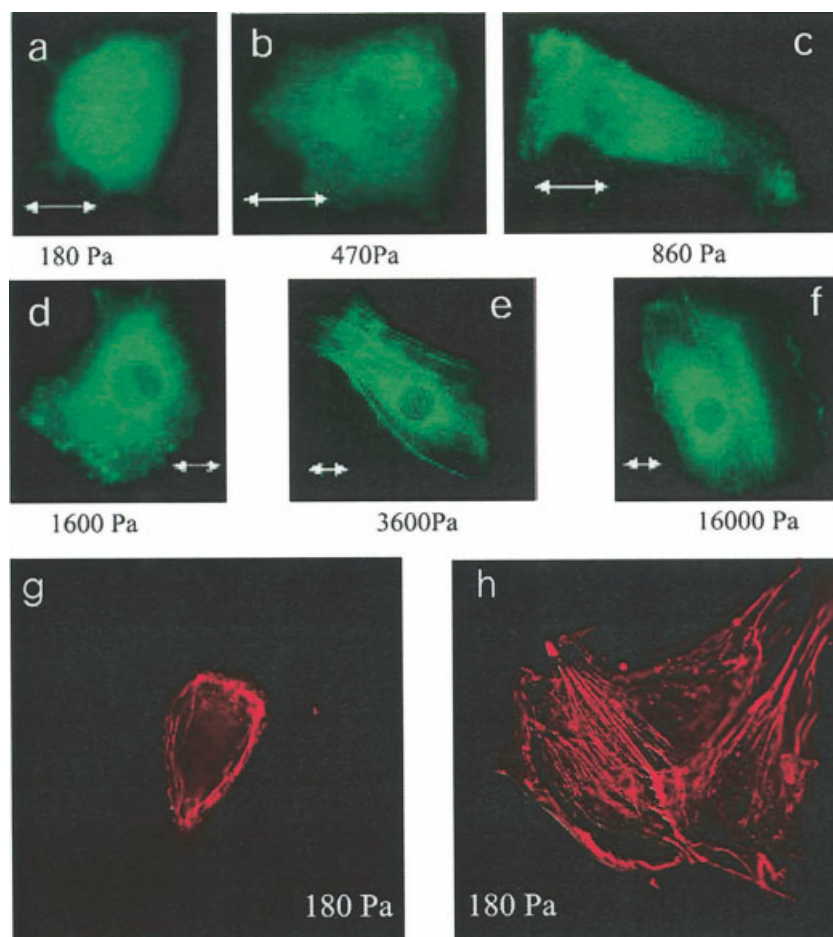


Fig. 2. Effect of substrate mechanical properties on fibroblast actin cytoskeleton. **a–f**: NIH 3T3 fibroblasts expressing EGFP-actin were plated on polyacrylamide gels with rigidities ranging from 180 Pa (a) to 16,000 Pa (f). Fibroblasts on soft materials had no stress fibers compared with fibroblasts on stiffer materials that do have articulated stress fibers. Scale bar = 10  $\mu$ m. **g,h**: NIH 3T3 fibroblasts on soft gels (180 Pa) are fixed with 4% paraformaldehyde and their F-actin stained with rhodamine phalloidin. The isolated fibroblast (g) appears to have no stress fibers as in a. When the fibroblasts are able to make cell-cell contact (h), stress fibers form. Scale bar = 15  $\mu$ m.

GFP-actin, fibroblasts grown on gels softer than 1,600 Pa had no detectable stress fibers or other actin bundles visible by fluorescence microscopy. At stiffnesses above 3,600 Pa, such actin fibers were a nearly universal feature of these cells.

The absence of stress fibers on soft gels was not an indication of toxicity since cell growth rates were only slightly slower on 180-Pa gels compared to the rates on the stiffest gels (55,000 Pa) and rates on gels between 1,600 and 3,600 Pa were equal to or greater than those on the stiffest gels. The absence of stress fibers was also only evident on single cells on the soft gels. As the cell density increased over time, cells that made cell-cell contact frequently became elongated and developed stress fibers. Figure 2g,h shows two examples of fibroblasts grown 48 h on a 180-Pa gel and stained with rhodamine phalloidin. The single cell (Fig. 2g) shows phalloidin staining consistent with the images of GFP-actin under these conditions showing amorphous F-actin distribution and no evidence of stress fibers. Comparable cells (Fig. 2h) on the same gel stiffness that had made intercellular contact show a more flattened morphology and abundant stress fibers.

A similar dependence of cell shape on stiffness was also seen with bovine aorta endothelial cells. These cells, shown after 1 day in culture in Figure 3, also ranged from round to well spread as the stiffness was increased about a few thousand Pa. As with fibroblasts, the round cells on soft surfaces were capable of division and were able to form confluent monolayers indistinguishable from those formed by cells on stiffer surfaces. Figure 3d–f shows monolayers developed after 3 days of culture on surfaces of stiffness varying from 180 to 29,000 Pa. Unlike the obvious difference in shape of single cells, these endothelial cells lose their morphologic difference once they make cell-cell contact. The density of cells in the monolayers also was independent of substrate stiffness, with 927, 898, and 895 adherent cells counted on equal-size areas ( $600 \times 490 \mu\text{m}$ ) of gels with elastic moduli of 180, 2,900, and 28,600 Pa, respectively.

The dependence of cell shape on stiffness is shown quantitatively in Figure 4. Figure 4a shows the average circumference of 3T3 fibroblasts grown for 1 day on gels of varying stiffness that were laminated with either fibronectin (circles) or type 1 collagen (triangles). The circumference of these cells changes by more than a factor of 4 as the

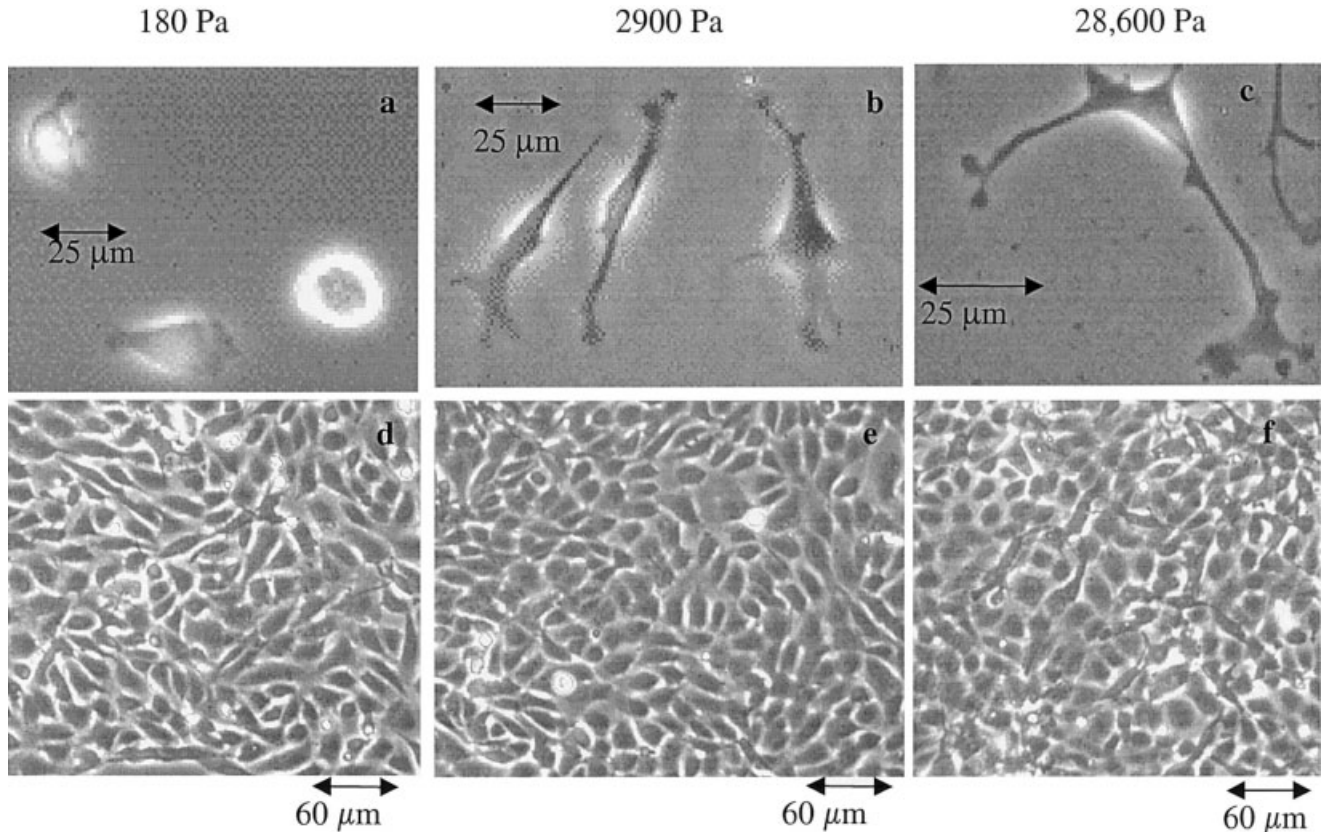


Fig. 3. Effect of substrate mechanical properties on endothelial cell morphology. Bovine aortic endothelial cells (BAECs) were plated on polyacrylamide gels. Projected cell area increases with substrate stiffness (a–c). As cells reach confluence (d–f) a monolayer forms in all groups and the morphologies become indistinguishable.

substrate stiffness increases and reached a value almost identical to that on glass for FN-laminated gels with stiffness above 10,000 Pa. On soft gels, 3T3 fibroblasts have approximately the same size when bound either to FN or collagen, but on gels with 10,000 Pa, they show more modest spreading on collagen than when bound to FN. Similar results were obtained when plotting adherent area instead of circumference (data not shown). Controls on glass could not be done for collagen since in this case FN from the serum-containing medium would also bind the glass surface and provide these cells with an additional adhesion protein. The non-monotonic dependence of circumference (or area) with gel stiffness is unexplained but apparently not simply an artifact of measuring mean areas of populations with a large variance, since in repeated studies using different fibroblast samples and gel preparations, maxima in cell spreading were seen at intermediate stiffnesses around 3,000 Pa.

Endothelial cells also show a stiffness-dependent spreading, but the change is not as large as for fibroblasts as quantified either by cell circumference (Fig. 4b) or area (data not shown). As with fibroblasts, spreading on collagen is somewhat less than on FN-coated gels.

In contrast to both fibroblasts and endothelial cells, human neutrophils exhibit no dependence of cell shape on substrate stiffness over the stiffness range accessible by this system. Figure 4c shows that the circumference of neutrophils is constant on gels with stiffness from 2 to 1,000 Pa and equal to that seen on glass. Moreover, the fMLP-stimulated increase in cell spreading is as large on the softest gel that could be made (2 Pa) as it is on glass.

The difference in morphology observed after prolonged incubation on gels with different stiffness arises initially from large differences in the rates of spreading after initial adhesion of cells to the surface. Figure 5 shows time courses of the spreading of two representative fibroblasts after initial binding to gels with stiffness of 180 (Fig. 5a) or 55,000 Pa (Fig. 5b). The change in adherent area with time for 5 such cells under each condition are shown in Figure 5C and D. There is a rather broad range of spreading rates under both conditions, but, on average, cells on soft gels do not spread fast or very far compared to cells on stiffer gels. On the stiff gels, a few cells fail to spread after

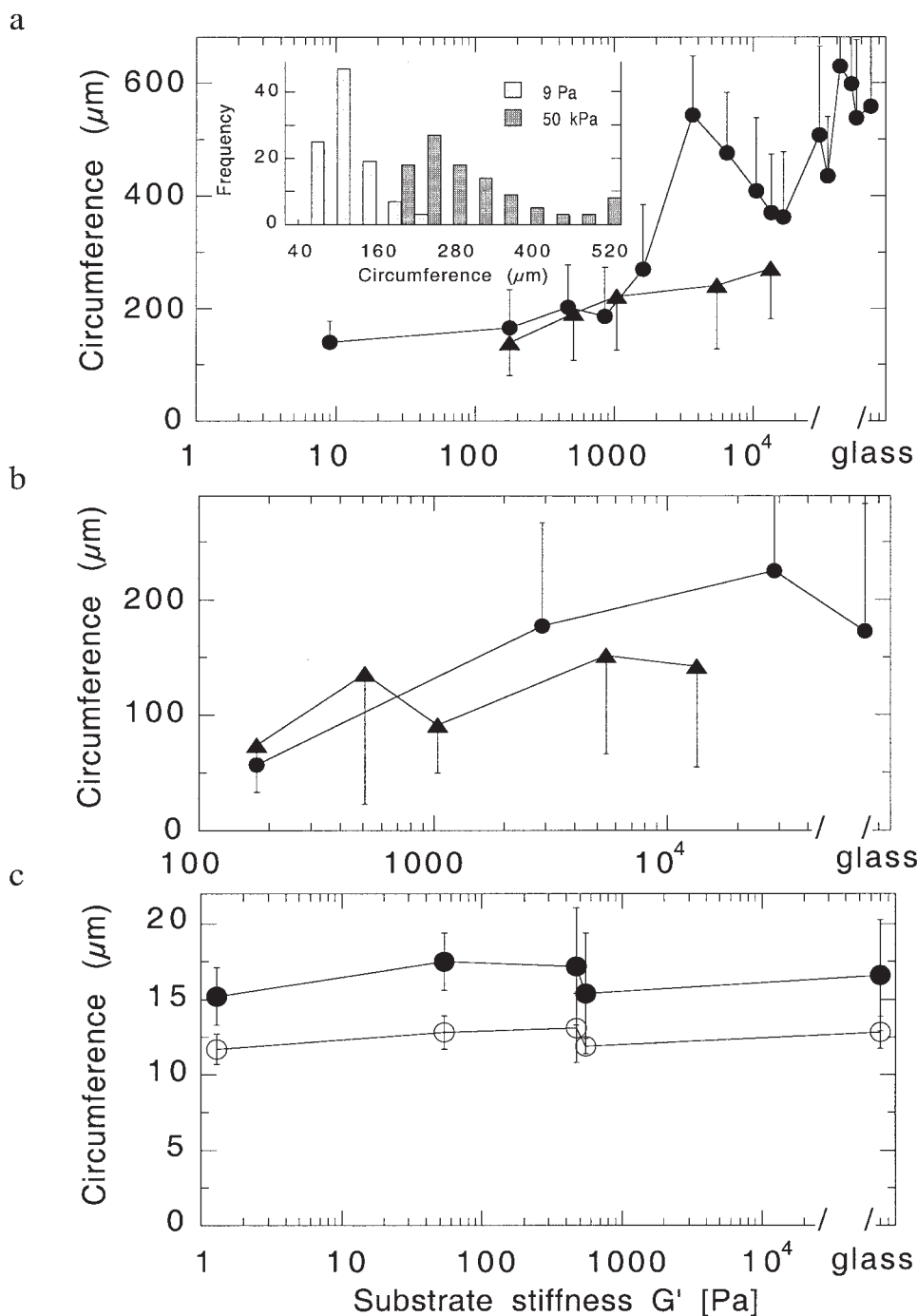


Fig. 4. Measurement of cell circumference for different cell types on substrates of varying rigidities. NIH 3T3 fibroblasts (a) and BAECs (b) were plated on flexible substrates coated with fibronectin (circles) or type I collagen (triangles) and imaged after 24 h in culture. Both fibroblasts and BAECs increased in circumference as substrate stiffness increased. Cells plated on fibronectin reached a larger apparent circumference than those plated on collagen. A histogram of circumference measurements (inset in a) shows that despite a large variation in cell circumference within a given cell population, the distributions measured at different stiffnesses overlap very little. Human blood neutrophils (c) were also plated on varying rigidities and left untreated (open circles) or stimulated (filled circles) with fMLP. Neutrophil circumference remains essentially stable despite gel stiffness. Error bars denote S.E.M. from measurements of 10 to 200 cells for each data point.

initial attachment but most spread at a rate never observed on the soft gel. The average rate of spreading as quantified by the initial rate of area versus time (Fig. 5c, inset) is more than 5 times larger on the stiffer gel.

Coincident with the rather abrupt spreading of fibroblasts on FN-coated surfaces stiffer than 2,000 Pa was a large increase in expression of  $\alpha 5$  integrin

(Fig. 6a). The increase in  $\alpha 5$  integrin expression on stiff gels may indicate an increase in adhesivity on stiffer materials. To determine if  $\alpha 5$  integrin expression was sufficient to cause cell spreading, even on soft surfaces, the  $\alpha 5$  subunit was expressed as an EGFP fusion in NIH 3T3 fibroblasts. The exogenous expression of EGFP- $\alpha 5$  had no obvious effect on cell spreading, as cells on soft and stiff gels followed the

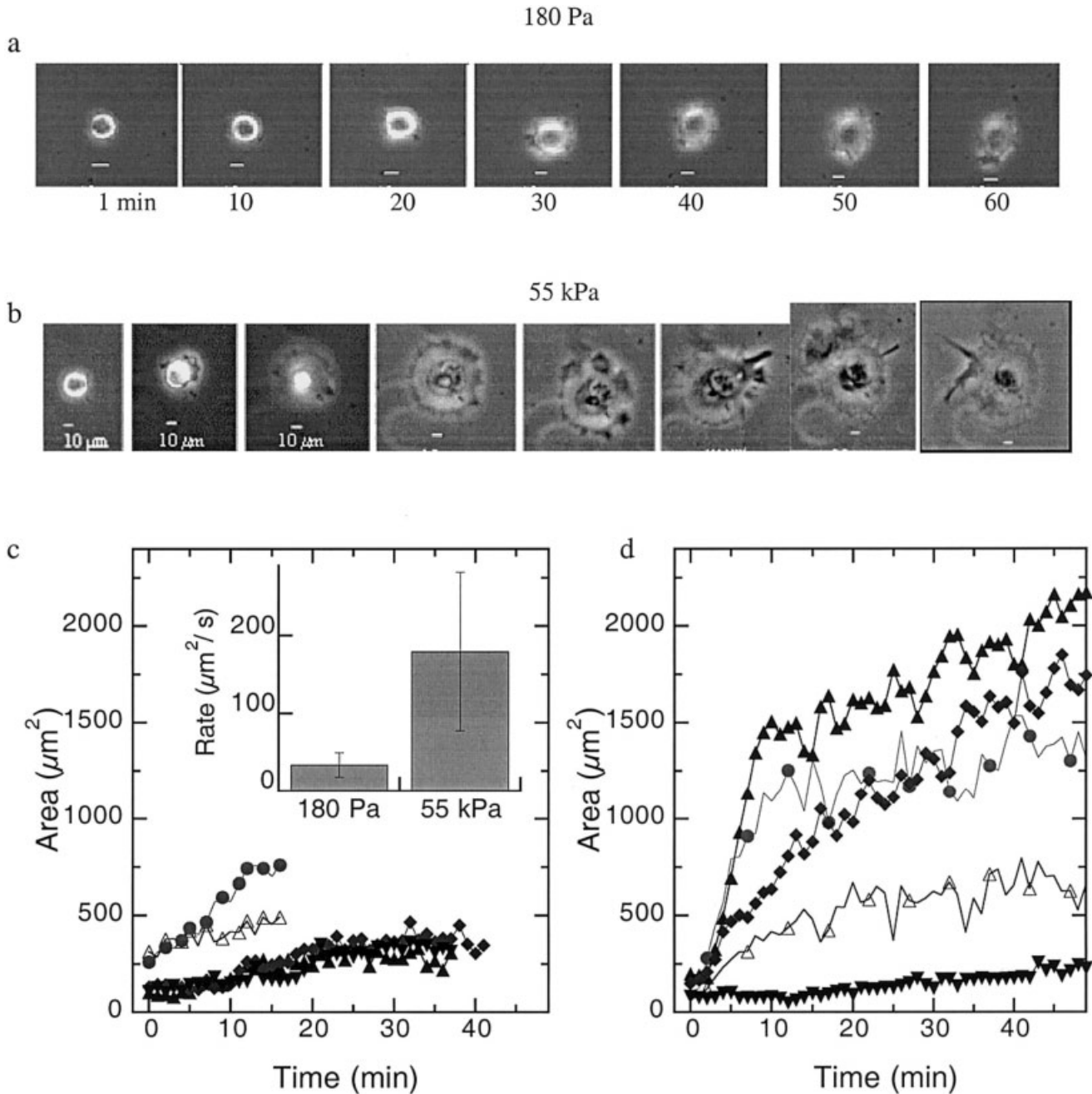


Fig. 5. Cell spreading dependence on substrate stiffness. The initial cell spreading as measured by cell area of NIH3T3 fibroblasts on soft (a,c) and stiff gels (b,d) shortly after plating. a,b: Representative phase images of fibroblasts spreading on both gels show that cells on soft gels (a) spread very little compared with the extent of spreading on stiff gels (b). Quantification of adherent cell area shows that cells on soft gels are smaller and exhibit a slower spreading rate (c) compared to the average of cells on stiff gels (d). **Inset** in c: Rate of spreading as quantified by initial rate of area versus time on soft and stiff gels.

same morphological trend as untransfected cells (Fig. 6b,c). On soft gels,  $\alpha 5$  was evident along the plasma membrane, but the cell did not spread as it did on stiff gels where the adherent area was larger and the  $\alpha 5$  had a punctate distribution.

## DISCUSSION

Most cell types in multicellular organisms are attached to soft materials, either other cells or extracellular matrices, but most of what is known about cell structure



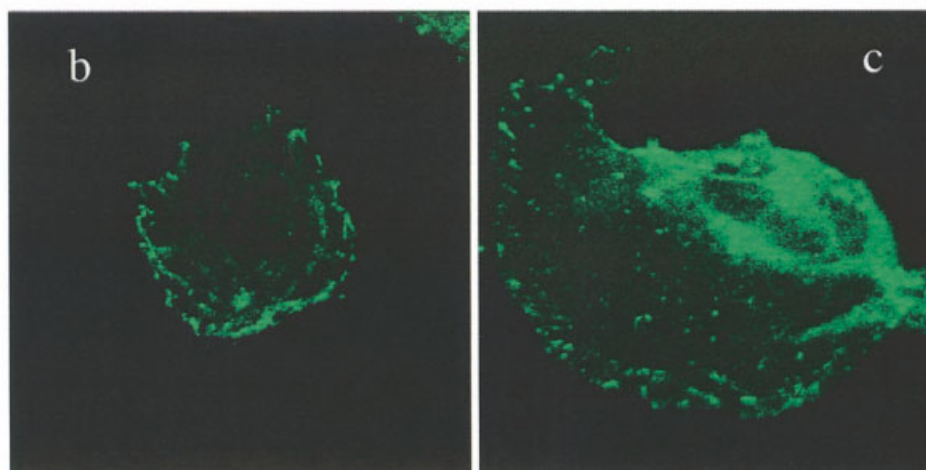
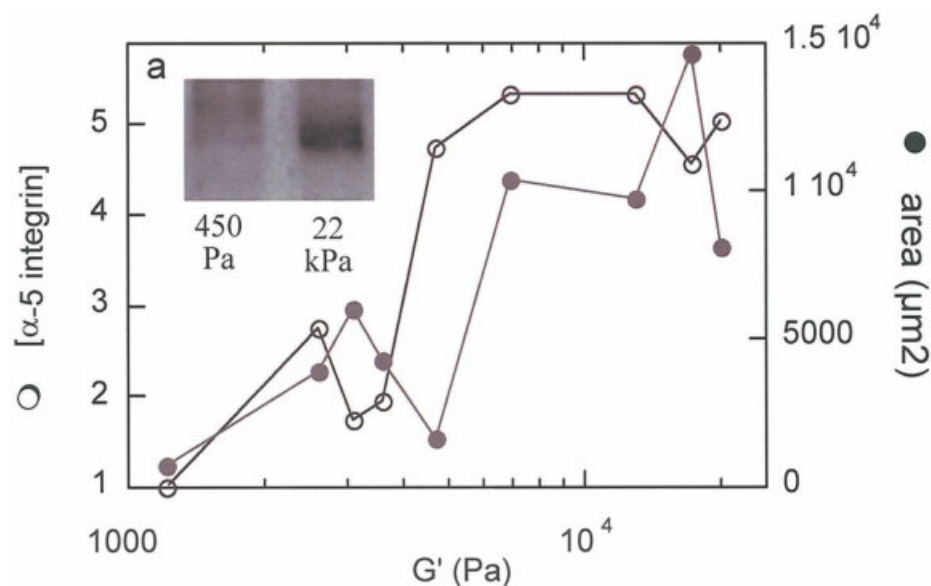


Fig. 6. Role of  $\alpha$ 5-integrin in fibroblasts on flexible substrates. **a:** Fibroblasts plated on varying rigidities were lysed after 24 h in culture, and  $\alpha$ 5 expression was determined by Western blot analysis as shown in the **inset**. Fibroblasts on stiff materials show a 5-fold increase in protein expression compared with cells on softer gels. **b,c:** Exogenous expression of  $\alpha$ 5 by transfection with GFP- $\alpha$ 5 had no effect on cell spreading. Cells on soft gels (**b**) showed that  $\alpha$ 5 was present and localized to the cell membrane, but cells remained small and rounded. In contrast, cells on stiff gels expressing exogenous  $\alpha$ 5 (**c**) were well spread.

and function *in vitro* derives from studies of cells plated on rigid substrates such as plastic or glass, laminated with a thin film of protein. As a result, some prominent aspects of cell structure, such as the fan-shaped morphology of cultured fibroblasts or the prevalence of large actin-containing stress fibers that are commonly studied *in vitro*, are rarely if ever seen *in vivo*. One well-recognized and studied reason to account for such differences is that many cell types *in vivo* function within a three-dimensional matrix, in contrast to the growth of cultured cells at a solid/liquid interface [Bard and Hay, 1975; Greenburg and Hay, 1982], but an additional independent difference relates to differences in elasticity of biological surfaces [Lo et al., 2000; Pelham and Wang 1997; Wang et al., 2000a]. The studies reported here show that cellular response to matrix stiffness may be very different

in different cell types and depends on the nature of the adhesion receptor by which the cell binds its substrate. There are also important differences between cells grown on two- and three-dimensional adhesive materials, but even when confined to adhesion on flat surfaces, the elastic constant of the surface can determine cell morphology and protein expression over a very wide range. Recent studies with aortic smooth muscle cells have shown that substrate stiffness is a more important determinant for cell shape than is the density of adhesive ligand to which the cell binds [Engler et al., 2004].

In addition to relatively well-recognized mechanical signals produced at cell-matrix adhesion sites, cells in mechanically active environments also form extensive, cadherin-mediated intercellular junctions that are important in tissue remodeling and differentiation. A relevant

finding in the work reported here is that when endothelial cells or fibroblasts make cell-cell junctions on soft substrates, they convert to the morphology seen on stiffer substrates. Specifically, fibroblasts in contact with other cells spread and develop stress fibers even on surfaces of 100-Pa stiffness, when neighboring single cells maintain a radically distinct rounded morphology (Fig. 2h). Likewise, endothelial cells when confluent have indistinguishable morphologies on soft and hard substrates while their structures are easily distinguishable when they are sparse enough to lack cell-cell junctions.

The simplest explanation for this change is that cells have a binary sensor at their membrane junction sites that signals for a relaxed rounded morphology when the surface is softer than the cell's intrinsic elastic modulus, and signals for another phenotype with increased contractility and stress fiber formation when the external material, either another cell or an extracellular matrix, is stiffer than the cell or as stiff as the cell itself. An alternate but not exclusive explanation is that the signals for mechanically induced morphologic differences come only from extracellular ligand-activated integrins, and that activated cadherins override these signals to establish a distinct program. Adherens junctions in connective tissue fibroblasts or other cell types may transmit mechanical signals and coordinate multicellular adaptations to physical forces [Ko et al., 2001; Nelson and Chen, 2003; Philippova et al., 1998]. The involvement of cadherin-based adhesions sites in sensing and responding to the mechanical properties of the tissue is strongly suggested by the finding that in wound healing, intercellular contacts involving interactions between cadherins, actin, and myosin are implicated in generating the forces required for wound closure [Adams and Nelson, 1998]. Notably, maintenance of the structure of intercellular contacts critically depends upon contractile forces generated by the actin cytoskeleton [Danjo and Gipson 1998] that act on intercellular contacts in adjacent cells [Gloushankova et al., 1998], and the magnitude and spatial distribution of these forces depend on the viscoelastic properties of the cells as well as the underlying matrix.

One clear outcome of these studies is that not all cells appear to use stiffness as a cue for morphology or motility, and the well-documented increase in spread area in fibroblasts [Lo et al., 2000] as matrix stiffness or density of adhesions sites increases is not universally observed. Figure 4, for example, shows that, unlike fibroblasts or endothelial cells, neutrophils appear to be insensitive to matrix stiffness. In the inactive state, they are relatively round on all surfaces tested and can spread and protrude after stimulation by a chemotactic peptide equally well on a gel with elastic modulus 2 Pa as they do on glass. The ability of neutrophils to spread on such a soft matrix is remarkable because it means that the cell extends its cortical actin-rich periphery without being

able to generate large traction forces that it can generate during phagocytosis [Evans et al., 1993] and that appear to be essential for extension of fibroblast cytoskeletons. Another example that runs counter to the expectation that cell protrusion requires traction forces exerted on a stiff material is observed with neurons derived from embryonic murine spinal cord. These cells extend processes that branch most effectively on soft surfaces with maximal branching on gels with stiffness of 50 Pa [Flanagan et al., 2002]. The detailed differences in how neutrophils and other cell types employ actin polymerization and acto-myosin contractility to move are not known, but they must be variable enough to allow robust spreading and motility of neutrophils and neurons on surfaces that are far too soft to allow fibroblasts or endothelial cells to spread. There are clearly defined differences in the number, size, and stability of integrin-based adhesions in different cell types [Entschladen and Zanker, 2000], and it seems probable that large focal adhesions characteristic of fibroblasts on stiff surfaces do not form nor could they function on soft gels [Balaban et al., 2001]. Different cell types may have adapted responses to different ranges of stiffness to match their function in vivo.

The magnitude of stiffness over which fibroblasts switch from being round and free of stress fibers to the fan-shaped form with abundant stress fibers seen when grown on rigid surfaces may help differentiate among different possible structures responsible for stiffness sensing. For fibroblasts on fibronectin-coated surfaces, the transition occurs around a value for the shear modulus of 1,000 to 3,000 Pa. This stiffness is similar to the elastic modulus of the fibroblast itself. Measurements by atomic force microscopy of Young's modulus (equal to 3 times the shear modulus for simple incompressible solids) of an NIH 3T3 fibroblasts on a rigid surface are between 3 and 12 kPa [Rotsch et al., 1999]. The similarity of these elastic constants suggests that fibroblasts may undergo spreading only when internally generated forces, which are reported to be independent of collagen matrix stiffness [Freyman et al., 2002], are exerted on a surface that is stiff enough so that the resulting deformation is partly within the cytoskeleton and not only within the external matrix.

The measured shear moduli of the polyacrylamide-based gels used in these studies is somewhat smaller than the elastic moduli reported from measurements of uniaxial extension or indentation reported in other studies. The forces that cells apply to a flat surface are shear forces, and therefore the shear modulus measured here is the relevant parameter quantifying resistance of the material to this geometry of force application. The Young's modulus, as measured by extensional or indentation methods, is related to the shear modulus by a function that requires knowledge of the Poisson's ratio of the material. The somewhat smaller values of shear modulus measured directly may help resolve

a question related to the mechanism by which cells produce the internal stress that allows them to probe matrix mechanical properties. Magnitudes of this stress, reported to be as large as 30 kPa in some studies, are difficult to account for by a purely acto-myosin dependent process because the concentration of cellular myosin and the known range of forces each motor can generate are not sufficient to produce this level of force per surface area, suggesting that other force-generating mechanisms such as osmotic stress may be involved. However, the relevant elastic constants may be smaller than those used to calculate internal stress, and the transition from round to spread morphology of fibroblasts shown in Figure 4 suggests that internal stresses of 3,000 Pa may be sufficient for mechanosensing.

## CONCLUSION

The stiffness of the surface to which cells adhere can have a profound effect on cell structure and protein expression, but these mechanical effects vary with different cell types, and depend on the nature of the adhesion receptors by which the cells bind their substrate. Fibroblasts and endothelial cells develop a spread morphology and actin stress fibers only when grown on surfaces with an elastic modulus greater than 2,000 Pa, with a greater effect seen when bound to fibronectin compared to collagen. In contrast, neutrophils appear to be insensitive to stiffness changes over a very wide range. The stiffness-dependence of fibroblasts and endothelial cells is no longer evident when cells become confluent, or in the case of fibroblasts even when two cells make contact suggesting either that mechanosensing uses the cells' internal stiffness as a criterion or else that signaling from cadherins in cell-cell contacts overrides signals from the cell-matrix adhesion complexes.

## REFERENCES

- Adams CL, Nelson WJ. 1998. Cytomechanics of cadherin-mediated cell-cell adhesion. *Curr Opin Cell Biol* 10:572–577.
- Balaban NQ, Schwarz US, Riveline D, Goichberg P, Tzur G, Sabanay I, Mahalu D, Safran S, Bershadsky A, Addadi L, Geiger B. 2001. Force and focal adhesion assembly: a close relationship studied using elastic micropatterned substrates. *Nat Cell Biol* 3:466–472.
- Bao G, Suresh S. 2003. Cell and molecular mechanics of biological materials. *Nat Mater* 2:715–725.
- Bard JB, Hay ED. 1975. The behavior of fibroblasts from the developing avian cornea. Morphology and movement in situ and in vitro. *J Cell Biol* 67:400–418.
- Cunningham CC, Vegners R, Bucki R, Funaki M, Korde N, Hartwig JH, Stossel TP, Janmey PA. 2001. Cell permeant polyphosphoinositide-binding peptides that block cell motility and actin assembly. *J Biol Chem* 276:43390–43399.
- Danjo Y, Gipson IK. 1998. Actin "purse string" filaments are anchored by E-cadherin-mediated adherens junctions at the leading edge of the epithelial wound, providing coordinated cell movement. *J Cell Sci* 111:3323–3332.
- Engler A, Bacakova L, Newman C, Hategan A, Griffin M, Discher D. 2004. Substrate compliance versus ligand density in cell on gel responses. *Biophys J* 86:617–628.
- Entschladen F, Zanker KS. 2000. Locomotion of tumor cells: a molecular comparison to migrating pre- and postmitotic leukocytes. *J Cancer Res Clin Oncol* 126:671–681.
- Evans E, Leung A, Zhelev D. 1993. Synchrony of cell spreading and contraction force as phagocytes engulf large pathogens. *J Cell Biol* 122:1295–1300.
- Flanagan LA, Ju YE, Marg B, Osterfield M, Janmey PA. 2002. Neurite branching on deformable substrates. *Neuroreport* 13:2411–2415.
- Flory P. 1953. Principles of polymer chemistry. Ithaca: Cornell University Press. 672 p.
- Freyman TM, Yannas IV, Yokoo R, Gibson LJ. 2002. Fibroblast contractile force is independent of the stiffness which resists the contraction. *Exp Cell Res* 272:153–162.
- Gloukhankova NA, Krendel MF, Alieva NO, Bonder EM, Feder HH, Vasiliev JM, Gelfand IM. 1998. Dynamics of contacts between lamellae of fibroblasts: essential role of the actin cytoskeleton. *Proc Natl Acad Sci USA* 95:4362–4367.
- Greenburg G, Hay ED. 1982. Epithelia suspended in collagen gels can lose polarity and express characteristics of migrating mesenchymal cells. *J Cell Biol* 95:333–339.
- Ko KS, Arora PD, McCulloch CA. 2001. Cadherins mediate intercellular mechanical signaling in fibroblasts by activation of stretch-sensitive calcium-permeable channels. *J Biol Chem* 276:35967–35977.
- Laukaitis CM, Webb DJ, Donais K, Horwitz AF. 2001. Differential dynamics of alpha 5 integrin, paxillin, and alpha-actinin during formation and disassembly of adhesions in migrating cells. *J Cell Biol* 153:1427–1440.
- Lo CM, Wang HB, Dembo M, Wang YL. 2000. Cell movement is guided by the rigidity of the substrate. *Biophys J* 79:144–152.
- Nelson CM, Chen CS. 2003. VE-cadherin simultaneously stimulates and inhibits cell proliferation by altering cytoskeletal structure and tension. *J Cell Sci* 116:3571–3581.
- Ory DS, Neugeboren BA, Mulligan RC. 1996. A stable human-derived packaging cell line for production of high titer retrovirus/viral stomatitis virus G pseudotypes. *Proc Natl Acad Sci USA* 93:11400–11406.
- Pelham RJ, Jr., Wang Y. 1997. Cell locomotion and focal adhesions are regulated by substrate flexibility. *Proc Natl Acad Sci USA* 94:13661–13665.
- Philippova MP, Bochkov VN, Stambolsky DV, Tkachuk VA, Resink TJ. 1998. T-cadherin and signal-transducing molecules co-localize in caveolin-rich membrane domains of vascular smooth muscle cells. *FEBS Lett* 429:207–210.
- Rossi FM, Guicherit OM, Spicher A, Kringstein AM, Fatyol K, Blakely BT, Blau HM. 1998. Tetracycline-regulatable factors with distinct dimerization domains allow reversible growth inhibition by p16. *Nat Genet* 20:389–393.
- Rotsch C, Jacobson K, Radmacher M. 1999. Dimensional and mechanical dynamics of active and stable edges in motile fibroblasts investigated by using atomic force microscopy. *Proc Natl Acad Sci USA* 96:921–926.
- Wakatsuki T, Kolodney MS, Zahalak GI, Elson EL. 2000. Cell mechanics studied by a reconstituted model tissue. *Biophys J* 79:2353–2368.
- Wang HB, Dembo M, Wang YL. 2000a. Substrate flexibility regulates growth and apoptosis of normal but not transformed cells. *Am J Physiol Cell Physiol* 279:C1345–C1350.
- Wang LZ, Gorlin J, Michaud SE, Janmey PA, Goddeau RP, Kuuse R, Uibo R, Adams D, Sawyer ES. 2000b. Purification of salmon clotting factors and their use as tissue sealants. *Thromb Res* 100:537–548.